



Seismic Rehabilitation of a Reinforced Concrete School in Northern Cyprus Following the 2023 Turkey Earthquake Sequences

Sasan BABAEI¹  Foad KARIMI GHALEH JOUGH^{1*} 

¹Faculty of Engineering, Department of Civil Engineering, Final International University, Via Mersin 10, AS 128, Kyrenia, Northern Cyprus

| Keywords | Abstract |
|--|---|
| Case Study Seismic Rehabilitation School Building Performance-Based Design Time History Analysis | In 2023, a 7.8-magnitude earthquake struck Turkey, causing severe damage to residential and critical infrastructure. In response, the government of the Turkish Republic of Northern Cyprus launched a program to rehabilitate educational facilities. This study examines the rehabilitation efforts at Atatürk Technical High School in Nicosia. A nonlinear time-history analysis was conducted to assess the building's seismic behavior, lateral load resistance, and plastic deformation during main shock and aftershock sequences. Shear walls and steel X-braced frames were subsequently integrated into the building's lateral load-resisting system, and their effectiveness was evaluated. The analysis indicated that the original structure would likely experience life safety risks and structural damage in vertical elements, with some parts at risk of collapse after the second loading sequence. In contrast, the rehabilitated structure demonstrated immediate occupancy performance, with no plastic hinge formation in either direction. The maximum roof displacement was also reduced to as little as one-third of that in the original structure. |

| Cite |
|--|
| Babaei, S., & Karimi Ghaleh Jough, F. (2025). Seismic Rehabilitation of a Reinforced Concrete School in Northern Cyprus Following the 2023 Turkey Earthquake Sequences. <i>GU J Sci, Part A, 12(1)</i> , 213-227. doi: 10.54287/guj.1590807 |

| Author ID (ORCID Number) | Article Process |
|--|-----------------------------------|
| 0000-0001-8672-5499 Sasan BABAEI | Submission Date 25.11.2024 |
| 0000-0003-0697-516X Foad KARIMI GHALEH JOUGH | Revision Date 10.12.2024 |
| | Accepted Date 07.01.2025 |
| | Published Date 26.03.2025 |

1. INTRODUCTION

On the morning of February 6, 2023, an earthquake with a magnitude of 7.8 struck south-central Turkey. Approximately nine hours later, a second earthquake of magnitude 7.5 hit a nearby area, with the epicenters of both quakes less than 100 kilometers apart. Together, these events led to the tragic loss of over 57,000 lives in Turkey and Syria. Additionally, the earthquakes affected approximately 16% of Turkey's population and destroyed nearly half a million apartments across the region. (Akar et al., 2024; Babaei & Karimi Ghaleh Jough, 2024)

The doublet seismic hazard also overwhelmed critical infrastructure, including roads and essential public facilities, which are crucial to be immediately occupied such as hospitals. Hospitals need to remain operational to provide urgent care to the injured, while schools, beyond protecting students during school hours, can also serve as shelters for displaced individuals in the aftermath of a disaster. Given these essential functions, the

*Corresponding Author, e-mail: fooad.karimi@final.edu.tr

construction and maintenance of such buildings must meet high safety standards. (Babaei et al., 2024; Dowell, 2023; Wang et al., 2023)

Scholars who inspected the affected region highlighted several reasons for the infrastructure failures, including outdated building codes, subpar material quality, poor implementation practices, and adverse soil and site conditions. For instance, Turan et al. (2024), assessing the failure mechanisms in Malatya, found that the second seismic shock significantly increased casualties in densely populated areas by collapsing already weakened buildings and exposing a lack of sufficient emergency shelter options. (Turan et al., 2024) Zengin and Aydin's (2023) investigation revealed that pre-2000 buildings had concrete strengths often less than one-third of their design values, sometimes as low as 4 MPa. (Zengin & Aydin, 2023)

Structural failures in Hatay were exacerbated by issues such as incomplete framing at two orthogonal axes, the presence of short columns, and multiple cantilevers on facades. (Altunsu et al., 2024; Doğan et al., 2024) While post-2000 structures showed more brittle failure modes—such as beam-column joint fractures, out-of-plane bending, and shear failures of walls and columns with high width-to-depth ratios—there were also cases of sliding shear wall failures, bond-slip failures in ribbed reinforcement, and tension failures in beams and slabs. (Vuran et al., 2024)

Onat et al. (2024) conducted an experimental and numerical analysis on a historical masonry mosque in Malatya, demonstrating the need for additional lateral stiffness and damping systems. (Karimi Ghaleh Jough & Golhashem, 2020; Karimi Ghaleh Jough, 2023; Onat et al., 2024) Meanwhile, Mohammadi et al.'s (2024) comprehensive assessment of 11 bridges in the affected areas of Turkey and Syria found damage such as failures in shear keys, back walls, I-girders, and buckling of lower flanges, with some bridges experiencing liquefaction that caused tilting and road settlement (Mohammadi et al., 2024). Qu et al. (2023) studied 5 base-isolated and 7 fixed-base hospitals in the impacted regions, finding that while base-isolated hospitals remained operational, fixed-base ones mostly lost immediate occupancy due to significant nonstructural damage. (Qu et al., 2023; Babaei et al., 2023)

In response to the 2023 Turkish earthquake, the government of the Turkish Republic of Northern Cyprus initiated a program to rehabilitate critical facilities, including schools, in several cities. An effective assessment, beyond conventional gravitational and seismic analysis, should consider the nonlinearity of element behaviors, the frequency content and duration of seismic excitation, and uncertainties in material properties, geometry, and loads within the analysis environment. This case study focuses on the rehabilitation process conducted for Atatürk Technical High School, located in the city of Nicosia. (Jough & Şensoy, 2016; Karimi Ghaleh Jough & Beheshti Aval, 2018; Babaei & Zarfam, 2019; Babaei et al., 2020; Jough et al., 2021; Babaei & Hosseini, 2023; Karimi Ghaleh Jough & Ghasemzadeh, 2023; 2024; Jough, 2024;)

In this study, the existing structure was initially analyzed using time-history analysis, simulating both the main seismic event and its aftershock sequence. The structural response in both the X and Y directions was recorded

at the end of each ground motion sequence to assess nonlinear behavior and evaluate the load resistance capacity of the system in each direction. Additionally, the rehabilitated models proposed by the author as part of the recommendations for the Northern Cyprus government were analyzed using the same time-history approach. A comparative analysis of the original and rehabilitated structures demonstrated that the rehabilitation techniques, whether through shear walls or braced frames, were effective. The structures now behave symmetrically in both orthogonal directions, showing uniform deformation, and can meet immediate occupancy requirements, even after subsequent seismic sequences. Furthermore, the maximum roof displacement in both directions was substantially reduced, to as low as one-third of the initial displacement.

2. DEFINITION OF THE INVESTIGATED BUILDINGS

The building analyzed in this study is a 40- to 50-year-old school located in the center of Nicosia, North Cyprus. It consists of six distinct blocks, each constructed at different times and following specific building codes and material guidelines. These blocks include the main building, Hairdressing School, Classroom Blocks, Atelier, and Kindergarten, as illustrated in Figure 1, which shows the school's different buildings.

This study focuses on the two-story main building, which itself is made up of three separate blocks—A, B, and C—each built at different times. Blocks A and B were constructed around the 1980s and feature similar columns and beams.



Figure 1. Atatürk Technical High School; **a)** Main building, **b)** Hairdressing School, **c)** Classroom Blocks, **d)** Atelier

Block C, however, was developed in two phases, with the initial construction occurring about 30 years ago and additional parts added less than 10 years ago. While Block C generally shares the same lateral load-

resisting system—concrete moment frames—as Blocks A and B, its more recent additions include columns and beams with distinctive dimensions.

Laboratory testing revealed that Blocks A and B share similar concrete quality, specifically a C16 grade, with a maximum compressive strength of 16 MPa. In contrast, Block C has C18 grade concrete, providing a slightly higher compressive strength of 18 MPa in its original sections. Although the newer sections in Block C may use even higher-strength concrete, a conservative assumption was made to treat the entire structure as built with C18 concrete. Site inspections also did not reveal any steel strength degradation due to corrosion of the rebars. These findings most closely correlate with the Turkish Standard TS 708 (1973) for reinforcement steel.

The rehabilitation process utilized the original plans and documents provided by the authorities. It is important to note that for the first two blocks, A and B, the plans aligned well with the actual structure, including accurate dimensions for columns, beams, slab thicknesses, and rebar numbers and sizes. However, Block C did not follow the official plans. As a result, the dimensions and orientation of Block C had to be redrawn to reflect the current structure accurately. The final plan view of the investigated building, comprising all three blocks, is shown in Figure 2. Block A, located on the left side, measures 11 by 26 meters; Block B, situated in the middle, measures 22 by 26 meters; and Block C, positioned on the right side, measures 20 by 45 meters.

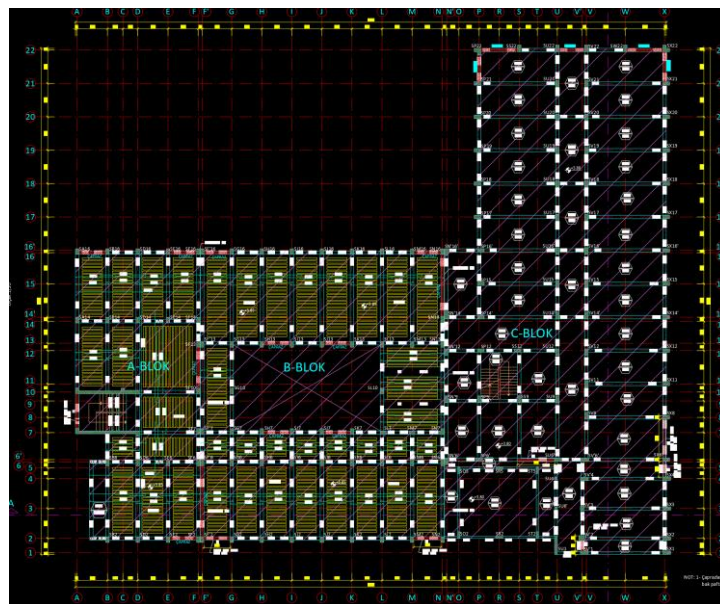


Figure 2. Plan view of the main building containing 3 blocks of A, B, and C

The dimensions and reinforcement of horizontal and vertical structural elements were obtained from the government's repository, as provided in Table 1. Figure 3 shows laboratory tests conducted to validate this information, revealing that the three blocks contain beams that are stronger than the columns, which is not ideal for building design. For optimal structural performance, the moment of inertia of the columns should be higher, allowing flexural deformations to occur in the horizontal elements (beams) rather than the vertical elements (columns). It should also be noted that Block A is the only block that incorporates a shear wall, positioned along the staircase and extending across the two-story structure.

Table 1. Dimensions and reinforcement properties of beam and columns

| Building | Element | Width (cm) | Height (cm) | Main Reinforcement | | | Stirrups |
|----------------------|----------|---------------|----------------|--------------------|-------------|-------------|-------------|
| | | | | Top | Middle | Bottom | |
| Block A | Column 1 | 30 | 50 | 2 ϕ 18 | 2 ϕ 18 | 2 ϕ 18 | ϕ 8@17 |
| & Block B | Beam 1 | 30 | 80 | 3 ϕ 18 | 2 ϕ 16 | 5 ϕ 18 | ϕ 8@15 |
| | Beam 2 | 30 | 80 | 4 ϕ 14 | 2 ϕ 14 | 4 ϕ 14 | ϕ 8@17 |
| Block C | Column 2 | 30 | 60 | 3 ϕ 18 | 4 ϕ 18 | 3 ϕ 18 | ϕ 8@17 |
| | Column 3 | 30 | 70 | 3 ϕ 18 | 4 ϕ 18 | 3 ϕ 18 | ϕ 8@17 |
| | Beam 3 | 30 | 50 | 2 ϕ 16 | 2 ϕ 16 | 2 ϕ 16 | ϕ 8@17 |
| | Beam 4 | 30 | 80 | 3 ϕ 18 | 2 ϕ 16 | 5 ϕ 18 | ϕ 8@17 |



Figure 3. Laboratory test for validation; a) Extracted concrete cores for compression test; b) Scanning concrete rebars

3. TIME HISTORY ANALYSIS

As indicated by the Ministry of Education, the rehabilitation technique was initially conducted using pushover analysis with three different software tools: ProtaStructure (Prota Software, 2018), SAP2000 (Computers and Structures, Inc., 2023, Version 24), and SeismoStruct (SeismoSoft, 2022). While pushover analysis is a reliable technique, it may not fully capture the nonlinear behavior of the structure, especially in response to the frequency content of seismic records. Additionally, pushover analysis cannot adequately represent the duration of ground motion or the sequence of hinge formation, as compared to time history analysis.

To evaluate the structure's seismic behavior, it was subjected to two sequences of strong ground motion from the 2023 Kahramanmaraş earthquake. The seismic sequence of the Pazarcık (Mw 7.7) and Elbistan (Mw 7.6) earthquakes, recorded at Station 4612 with a maximum peak ground acceleration of 0.52g, is shown in Figure 4. To account for plastic deformations and hinge formation in primary elements, specifications were applied

based on Table 10.8 and Table 10.9 of ASCE 41-17 for columns, and Table 10.7 for flexural elements. (ASCE/SEI 41/17, 2017) These specifications were incorporated into the structure using hinge definitions provided in SAP2000.

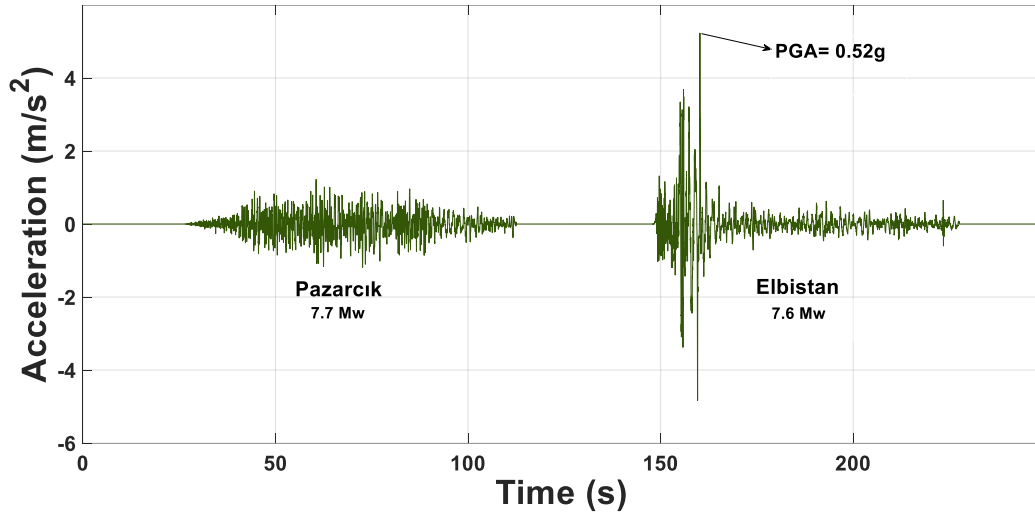


Figure 4. Acceleration-time history of Pazarcik (7.7Mw) and Elbistan (7.6Mw) ground motions from Station 4612 (AFAD, 2024)

An analysis of Block A shows that the structure remained elastic in both directions during the first sequence of ground motion. However, during the second sequence, known as the Elbistan earthquake, hinges began to form in primary elements, specifically the columns. Figure 5a and 5b display the deformation of Block A in the X and Y directions. In the X direction, where shear walls are incorporated around the staircase, the structure demonstrated high resistance, with only one hinge reaching the life safety level. In contrast, columns in the Y direction sustained significant damage: ten columns reached the life safety state, three columns reached the collapse prevention state, and nine columns experienced total collapse, as shown in Table 2. Notably, none of the beams in the structure failed, likely due to their large cross-sectional dimensions of 30 by 80 cm, which provide high moments of inertia and enhance flexural capacity. Additionally, the beams were reinforced with sufficient longitudinal rebar, enabling them to exhibit ductile behavior.

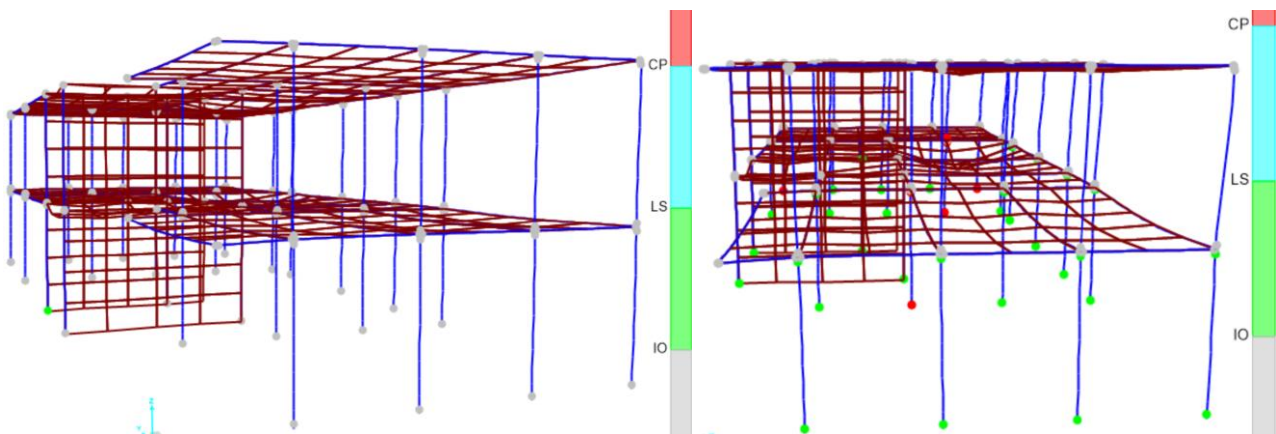
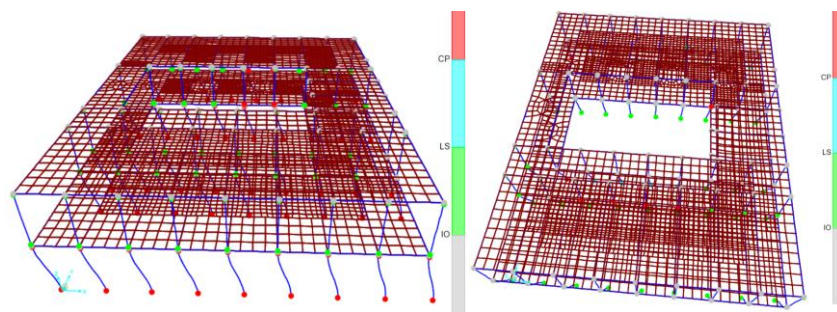


Figure 5. Hinge formations in the frames of block A at the end of the seismic sequence; a) X direction, b) Y direction

Table 2. Summary of the hinge formation in the frames of block A

| Direction | Element | Immediate occupancy | Life Safety | Collapse prevention | Collapse |
|-----------|---------|---------------------|-------------|---------------------|----------|
| X | Beams | 76 | 0 | 0 | 0 |
| | Columns | 49 | 1 | 0 | 0 |
| Y | Beams | 76 | 0 | 0 | 0 |
| | Columns | 19 | 19 | 3 | 9 |

Figure 6 illustrates the seismic behavior of the second block, Block B, in both the X and Y directions after the completion of the second ground motion sequence, as indicated in Table 3. None of the primary or secondary elements—namely, columns and beams—experienced hinge formation after the first sequence. However, as the intensity of the second ground motion increased, 38 columns reached the life-safety state, while 52 columns approached a collapse state in the X direction. Notably, none of the columns remained in the immediate occupancy category. In the Y direction, similar behavior was observed but with less severe damage: 25 columns remained in immediate occupancy, 51 reached the life-safety threshold, 4 were at collapse prevention, and 10 were in a collapse state. This analysis indicates that the structure in both the X and Y directions lacks sufficient lateral resilience to sustain these ground motions. Reinforcement techniques are recommended in both directions, particularly in the X direction, where a greater number of columns failed. Similar to Block A, none of the beams in Block B experienced hinge formation, likely due to their larger cross-section dimensions of 30 by 80 cm.

**Figure 6.** Hinge formations in the frames of block B at the end of the seismic sequence; a) X direction, b) Y direction**Table 3.** Building's blocks Columns and beams dimensions and reinforcements

| Direction | Element | Immediate occupancy | Life Safety | Collapse prevention | Collapse |
|-----------|---------|---------------------|-------------|---------------------|----------|
| X | Beams | 148 | 0 | 0 | 0 |
| | Columns | 0 | 38 | 0 | 52 |
| Y | Beams | 148 | 0 | 0 | 0 |
| | Columns | 25 | 51 | 4 | 10 |

Unlike the other two blocks, Block C experienced hinge formation even after the first seismic sequence in the Y direction. However, in the X direction, none of the structural elements experienced hinge formation,

allowing the structure to remain in immediate occupancy. Figure 7 illustrates that, after the second sequence of ground motion, 113 columns in the X direction reached the life-safety stage, with only one column reaching the collapse state.

In the Y direction, as shown in Figure 8, even after the first seismic sequence, 57 columns reached the life-safety stage, 23 columns were at collapse prevention, and 29 columns reached collapse. This damage intensified with the second sequence: only 6 columns remained in immediate occupancy, 56 reached the life-safety stage, 10 were at collapse prevention, and a significant 48 columns reached collapse.

It is also noteworthy that, unlike the columns, none of the beams in either the X or Y direction experienced hinge formation; all beams remained in immediate occupancy, likely due to their large cross-sectional dimensions, as shown in Table 4.

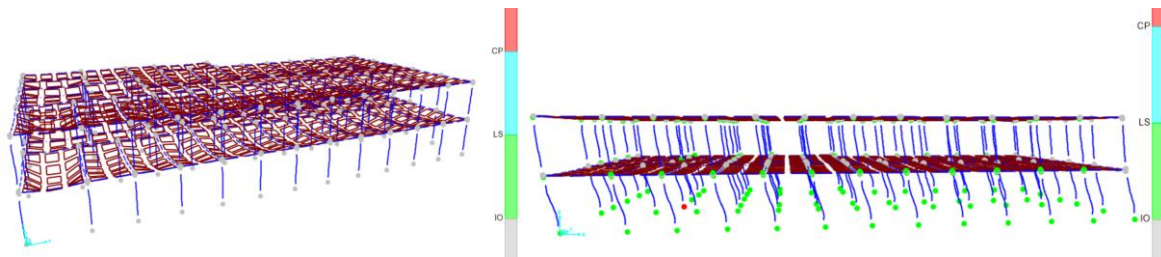


Figure 7. Hinge formations in the frames of block C at the X direction at the end of the; a) mainshock, b) aftershock

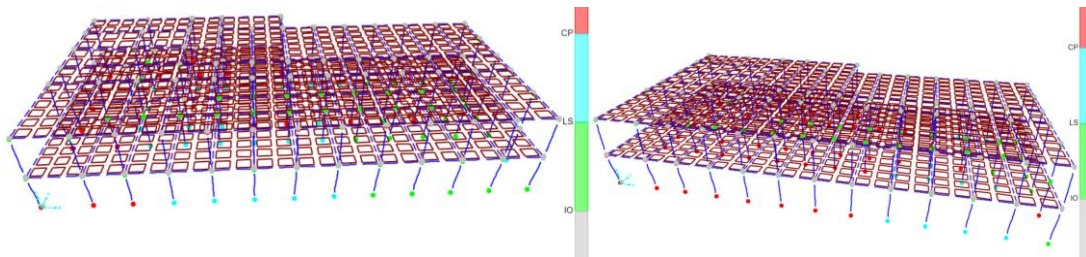


Figure 8. Hinge formations in the frames of block C at the Y direction at the end of the; a) mainshock, b) aftershock

Table 4. Summary of the hinge formation in the frames of the block C

| Direction | Record | Element | Immediate occupancy | Life safety | Collapse prevention | Collapse |
|-----------|--------|---------|---------------------|-------------|---------------------|----------|
| X | MS | Beams | 180 | 0 | 0 | 0 |
| | | Columns | 120 | 0 | 0 | 0 |
| | MS+AS | Beams | 180 | 0 | 0 | 0 |
| | | Columns | 6 | 113 | 0 | 1 |
| Y | MS | Beams | 180 | 0 | 0 | 0 |
| | | Columns | 11 | 57 | 23 | 29 |
| | MS+AS | Beams | 180 | 0 | 0 | 0 |
| | | Columns | 6 | 56 | 10 | 48 |

4. REHABILITATION TECHNIQUE

Structural analysis in both directions indicates that rehabilitation is necessary, corroborating earlier findings from the author's pushover analysis. The proposed rehabilitation methods include adding a 25-centimeter-thick C30 shear wall or an X-braced frame with sections measuring 200 cm in width and 10 cm in thickness. ST275-grade steel was selected as the material for the braces to enhance structural performance.

The rehabilitated model of the building, created using SAP2000 and ProtaStructure software, is depicted in Figure 9. As shown, X-direction brace frames were added to both the upper and lower portions of the structure, and two additional brace frames were incorporated along the Y direction on both sides. The purpose of positioning these brace frames at the edges of the structure in both X and Y directions is to mitigate unwanted rotational modes, enhancing overall stability. This configuration also facilitates additional foundation rehabilitation as needed.

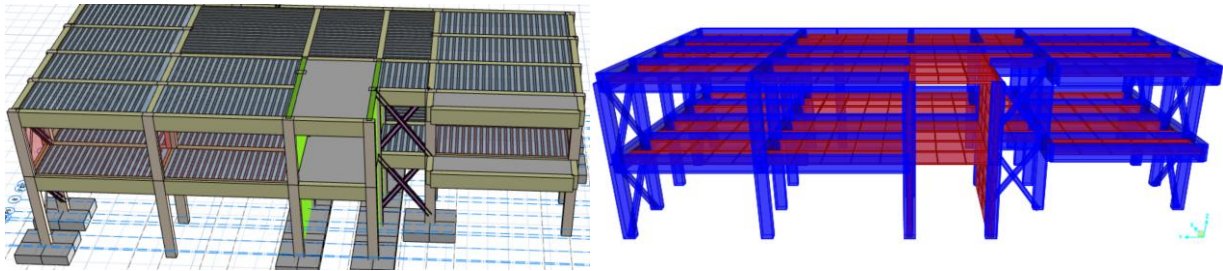


Figure 9. Rehabilitated building block A, a) Protastructure, b) SAP

Further modifications to the rehabilitated model are presented in Figure 10, focusing specifically on Block B. Two shear walls were introduced at the bottom side of the building, and two brace frames were incorporated at the top. In the building's inner core, which contains an opening, four brace frames were added in the X direction and another four in the Y direction to improve lateral stability.

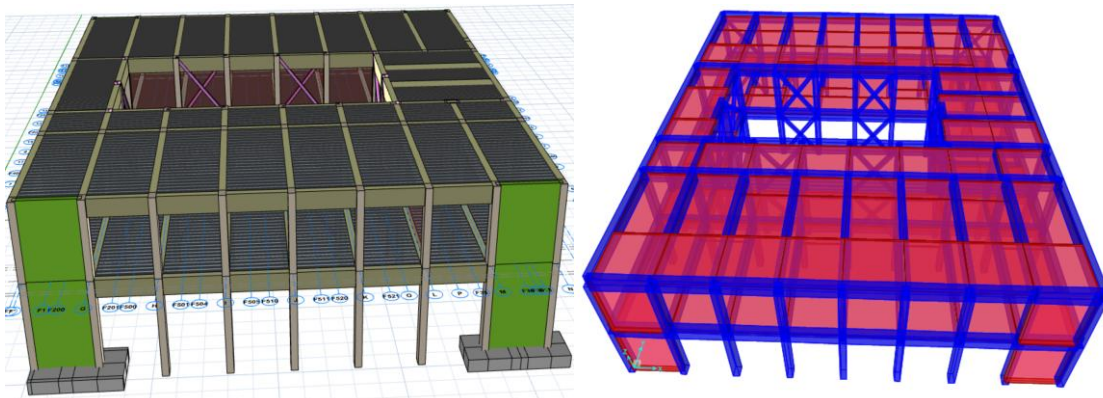


Figure 10. Rehabilitated building block B, a) Protastructure, b) SAP

As detailed in Figure 11, additional rehabilitation measures were applied in Block C. Two brace frames were installed at the front of the structure in both the X and Y directions, with additional reinforcement on the opposite side of the structure at the base. This included two shear walls in the X direction and two in the Y direction, incorporated to enhance the building's lateral load-resisting capabilities.

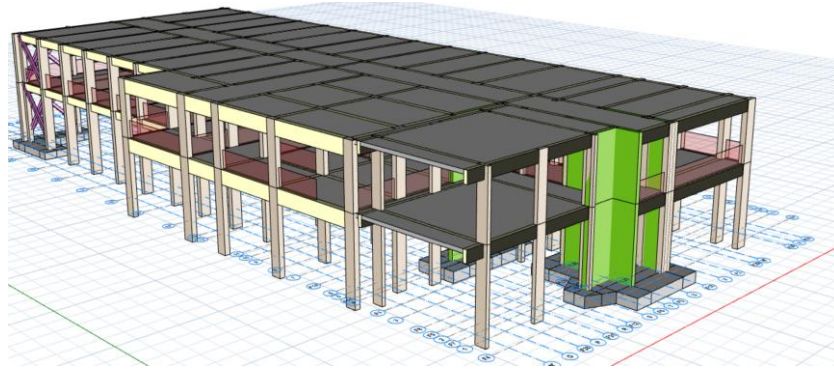


Figure 11. Rehabilitated building block C

Figure 12 and 13 illustrate the implementation of 25-centimeter shear walls and X-brace frames incorporated into the structure.



Figure 12. Shear wall added to block A; **a)** wall demolishing, **b)** Concrete pouring



Figure 13. X-braced frames added to block C; **a)** wall demolishing, **b)** Braced frame implementation **c)** Tube 200x200x12.5

5. COMPARISON OF THE EXISTING AND REHABILITATED BUILDINGS

Blocks A, B, and C experience no hinge formation, even after the second sequence in both directions, indicating sufficient structural ductility and seismic capacity. To compare this capacity more effectively, both the existing and rehabilitated buildings were subjected to a mainshock-aftershock sequence. Figure 14 shows the maximum roof displacement in the X and Y directions. In the X direction, the existing and rehabilitated

buildings demonstrate similar behavior, while in the Y direction, the rehabilitated building significantly reduces the maximum roof displacement.

Specifically, in Block A, the maximum roof displacement in the X direction decreased from 0.38 cm to 0.2 cm in the rehabilitated building. In the Y direction, displacement in Block A was reduced from 3.39 cm to 1.4 cm after rehabilitation, demonstrating a considerable improvement. This increased efficiency in the Y direction is attributed to the addition of braced frames, which significantly enhances lateral resistance. In contrast, the X direction already had sufficient resistance due to the existence of large shear walls, even before the rehabilitation.

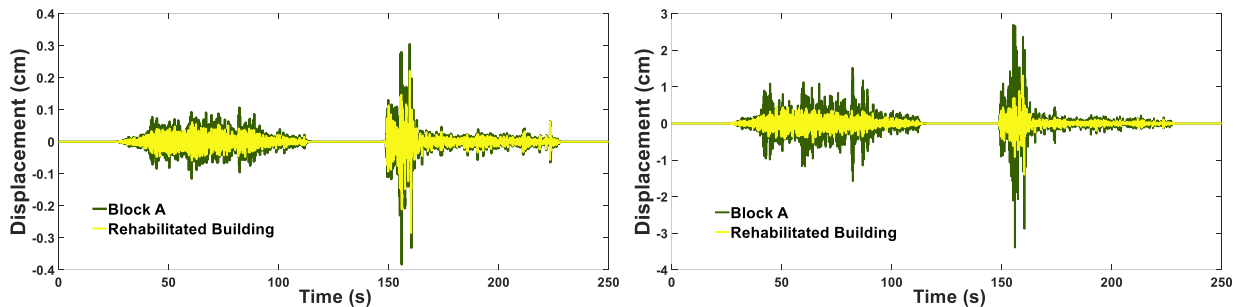


Figure 14. Time history analysis of Block A; a) X direction, b) Y direction

Figure 15 illustrates the structural behavior of the building under a nonlinear dynamic analysis. As shown, the non-rehabilitated structure was significantly impacted by the second sequence, with several elements yielding due to prior stress. This led to an increase in displacement amplitude during the second sequence in both the X and Y directions, particularly in the X direction. In contrast, the rehabilitated structure exhibits a more symmetrical response in both the X and Y directions and a stable response to ground motion, with no extreme displacement peaks following the second sequence.

As detailed in Table 5, the maximum roof displacement in the X direction decreased from 2.19 cm to 0.66 cm after rehabilitation. Similarly, in the Y direction, the maximum roof displacement was reduced from 1.16 cm to 0.22 cm. These improvements underscore the effectiveness of the rehabilitation measures in enhancing the building's seismic performance.

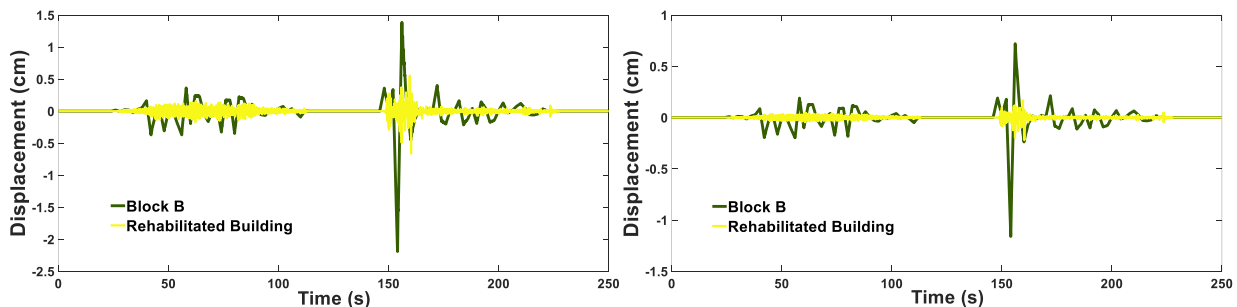


Figure 15. Time history analysis of Block B; a) X direction, b) Y direction

Figure 16 further illustrates the seismic behavior of both the non-rehabilitated and rehabilitated structures in Block C. As shown, the maximum roof displacement is significantly reduced in both the X and Y directions after rehabilitation. Specifically, in the X direction, the maximum roof displacement decreased from 3.31 cm to 1.5 cm—a reduction by more than half. In the Y direction, it was reduced from 3.67 cm to 1.32 cm, almost one-third of the original displacement. This improvement enhances the structure's natural resistance to severe earthquake impacts.

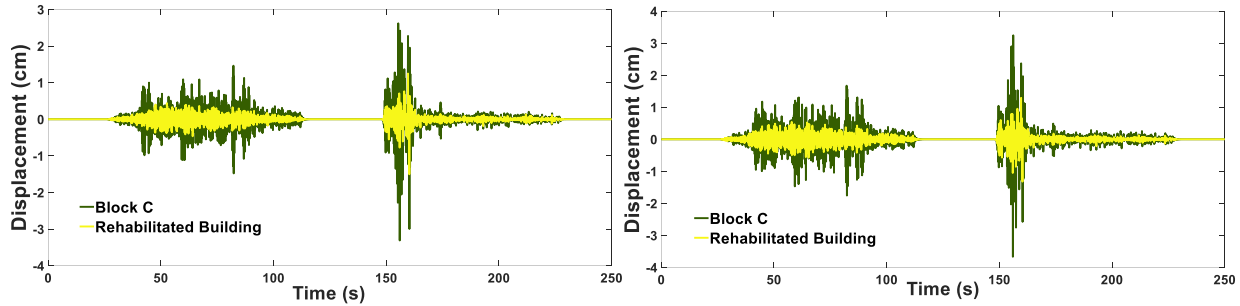


Figure 16. Time history analysis of Block C; a) X direction, b) Y direction

Table 5 shows that the two structures now exhibit much closer predominant mode shapes and periods, with the first modes in both the X and Y directions now aligned. Any rotational modes are effectively prohibited. Additionally, it should be noted that making the structure stiffer—either by adding shear walls or braced frames—has reduced the periods of the rehabilitated building compared to the non-rehabilitated one.

Table 5. Dynamic characteristics and seismic response of existing and rehabilitated building's blocks

| Building | Direction | Block A | | Block B | | Block C | |
|-----------------------------------|-----------|----------|---------------|----------|---------------|----------|---------------|
| | | Existing | Rehabilitated | Existing | Rehabilitated | Existing | Rehabilitated |
| Period (s) | X | 0.09 | 0.086 | 0.348 | 0.124 | 0.264 | 0.176 |
| | Y | 0.27 | 0.187 | 0.247 | 0.079 | 0.283 | 0.196 |
| Max Roof Displacement (cm) | X | 0.38 | 0.28 | 2.19 | 0.66 | 3.31 | 1.50 |
| | Y | 3.39 | 1.40 | 1.16 | 0.22 | 3.67 | 1.32 |

6. CONCLUSION

This case study examines the effectiveness of rehabilitation techniques applied to a structure located in Nicosia, Turkish Republic of Northern Cyprus. The complex consists of six buildings, with the main building selected for a time-history analysis based on the 2023 two-sequence Kahramanmaraş ground motions. This main building is divided into three distinct blocks: Block A, Block B, and Block C. A nonlinear time-history analysis was initially conducted to assess the performance of each block in the orthogonal X and Y directions. Findings reveal that, without rehabilitation, these buildings face life safety issues, hinge formation, and the potential for collapse by the end of the second sequence. However, when rehabilitation techniques—such as adding a 25-centimeter shear wall or hollow tube steel sections—are implemented to strengthen the lateral load-resisting system, the structures achieve immediate occupancy performance in both directions. The rehabilitated

buildings also experience a significant reduction in maximum roof displacement, to as little as one-third of the original structure's displacement. Additionally, the rehabilitated buildings exhibit symmetric behavior, with the X and Y direction mode shapes closely aligned as the dominant first and second modes.

AUTHOR CONTRIBUTIONS

Conceptualization, S.B.; methodology, S.B. and F.K.G.; fieldwork, S.B.; software, S.B.; title, S.B., and F.K.G.; validation, S.B.; laboratory work, S.B.; formal analysis, S.B. and F.K.G.; research, S.B.; sources, S.B.; data curation, S.B.; manuscript-original draft, S.B.; manuscript-review and editing, S.B. and F.K.G.; visualization, S.B. and F.K.G.; supervision, S.B. and F.K.G.; project management, S.B.; All authors have read and legally accepted the final version of the article published in the journal.

CONFLICT OF INTEREST

The authors declare no conflict of interest.

REFERENCES

- AFAD (2024). Republic of Turkey Ministry of Interior, Disaster and Emergency Management Presidency (AFAD) "Training and Awareness Department". Accessed: 24.02.2024, [URL](#)
- Akar, F., Işık, E., Avcil, F., Büyüksaraç, A., Arkan, E., & İzol, R. (2024). Geotechnical and Structural Damages Caused by the 2023 Kahramanmaraş Earthquakes in Gölbaşı (Adıyaman). *Applied Sciences*, 14(5).
- Altunsu, E., Güneş, O., Öztürk, S., Sorosh, S., Sarı, A., & Beeson, S. T. (2024). Investigating the structural damage in Hatay province after Kahramanmaraş-Türkiye earthquake sequences. *Engineering Failure Analysis*, 157, 107857. <https://doi.org/10.1016/j.engfailanal.2023.107857>
- ASCE/SEI 41/17. (2017). Seismic Evaluation and Retrofit of Existing Buildings. American Society Of Civil Engineers.
- Babaei, S., Habib, A., Hosseini, M., & Yildirim, U. (2024). *Investigating the Inelastic Performance of a Seismic Code-Compliant Reinforced Concrete Hospital Under Long Sequence of Ground Motions Records*. In: Proceedings of 15th International Congress on Advances in Civil Engineering (ACE2023) (pp. 364-373). https://doi.org/10.1007/978-981-97-1781-1_34
- Babaei, S., & Hosseini, M. (2023). Semi-active Control of 3D-Vertically Isolated Buildings with Divided Skeleton into Inner and Outer Interactive Subsystems Equipped with MR Dampers Canadian Conference - Pacific Conference on Earthquake Engineering 2023.
- Babaei, S., & Karimi Ghaleh Jough, F. (2024). A Comprehensive Evaluation of Tuned Vertical Isolation System for Seismic Risk Mitigation. *Journal of Applied Engineering Sciences*, 14(1), 27-34. <https://doi.org/10.2478/jaes-2024-0004>
- Babaei, S., & Zarfam, P. (2019). Optimization of shape memory alloy braces for concentrically braced steel braced frames. *Open Engineering*, 9(1), 697-708. <https://doi.org/10.1515/eng-2019-0084>

- Babaei, S., Zarfam, P., & Sarvghad Moghadam, A. (2020). Probabilistic and Deterministic Semi-Active Control Strategies for Adjacent Buildings Connected by MR Dampers 17th World Conference on Earthquake Engineering.
- Babaei, S., Zarfam, P., Sarvghad Moghadam, A., & Zahrai, S. M. (2023). Assessment of a dual isolation system with base and vertical isolation of the upper portion. *Structural Engineering and Mechanics*, 88(3), 263-271. <https://doi.org/10.12989/sem.2023.88.3.263>
- Computers and Structures, Inc. (2023). SAP2000 Integrated Software for Structural Analysis and Design (Version 24). Berkeley, CA: Computers and Structures, Inc. Available at: [URL](#)
- Doğan, T. P., Kalkan, H., Aldemir, Ö., Ayhan, M., Böcek, M., & Anıl, Ö. (2024). Investigation of RC structure damages after February 6, 2023, Kahramanmaraş earthquake in the Hatay region. *Bulletin of Earthquake Engineering*, 22(10), 5201-5229. <https://doi.org/10.1007/s10518-024-01965-2>
- Jough, F. K. G. (2024). Fuzzy Logic-Based Fragility Curve Development for Steel Moment-Resisting Frames Considering Uncertainties in Seismic Response. *Journal of Earthquake and Tsunami*, 18(05), 2450014. <https://doi.org/10.1142/S1793431124500143>
- Jough, F. K. G., & Şensoy, S. (2016). Prediction of seismic collapse risk of steel moment frame mid-rise structures by meta-heuristic algorithms. *Earthquake Engineering and Engineering Vibration*, 15(4), 743-757. <https://doi.org/10.1007/s11803-016-0362-9>
- Jough, F. K. G., Veghar, M., & Beheshti-Aval, S. B. (2021). Epistemic Uncertainty Treatment Using Group Method of Data Handling Algorithm in Seismic Collapse Fragility. *Latin American Journal of Solids and Structures*, 18.
- Dowell, K. (2023). Reconnaissance Report of Observed Structural Bridge Damage (SDSU STRUCTURAL ENGINEERING RESEARCH PROJECT, Issue.)
- Karimi Ghaleh Jough, F. (2023). The contribution of steel wallposts to out-of-plane behavior of non-structural masonry walls. *Earthquake Engineering and Engineering Vibration*, 22(1), 243-262. <https://doi.org/10.1007/s11803-023-2161-4>
- Karimi Ghaleh Jough, F., & Beheshti Aval, S. B. (2018). Uncertainty analysis through development of seismic fragility curve for an SMRF structure using an adaptive neuro-fuzzy inference system based on fuzzy C-means algorithm. *Scientia Iranica*, 25(6), 2938-2953. <https://doi.org/10.24200/sci.2017.4232>
- Karimi Ghaleh Jough, F., & Ghasemzadeh, B. (2024). Uncertainty Interval Analysis of Steel Moment Frame by Development of 3D-Fragility Curves Towards Optimized Fuzzy Method. *Arabian Journal for Science and Engineering*, 49(4), 4813-4830. <https://doi.org/10.1007/s13369-023-08223-8>
- Karimi Ghaleh Jough, F., & Ghasemzadeh, B. (2023). Reliability Prediction of SMRF Based on the Combination of Neural Network And Incremental Dynamic Analysis [SMRF'nin Sinir Ağı ve Artımlı Dinamik Analizin Birleşimine Dayanan Güvenilirlik Tahmini]. *Journal of Innovations in Civil Engineering and Technology*, 5(2), 91-105. <https://doi.org/10.60093/jiciviltech.1317804>

- Karimi Ghaleh Jough, F., & Golhashem, M. (2020). Assessment of out-of-plane behavior of non-structural masonry walls using FE simulations. *Bulletin of Earthquake Engineering*, 18(14), 6405-6427. <https://doi.org/10.1007/s10518-020-00932-x>
- Mohammadi, N. K., Yasuko; Akyol, E. (2024). Observed structural bridge damage report for the 2023 Turkey-Syria earthquake. Kobe University Research Center for Urban Safety.
- Onat, O., Özmen, A., Özdemir, E., & Sayın, E. (2024). Damage propagation and failure mechanism of single dome historical Masonry Mosque after February 6, 2023, Kahramanmaraş earthquake doublets ($M_w = 7.7$ and $M_w = 7.6$). *Structures*, 69, 107288. <https://doi.org/10.1016/j.istruc.2024.107288>
- Prota Software. (2018). ProtaStructure: Structural Design and Analysis Software. Available at: <URL>
- Qu, Z., Wang, F., Chen, X., Wang, X., & Zhou, Z. (2023). Rapid report of seismic damage to hospitals in the 2023 Turkey earthquake sequences. *Earthquake Research Advances*, 3(4), 100234. <https://doi.org/10.1016/j.eqrea.2023.100234>
- SeismoSoft. (2022). SeismoStruct: A Finite Element Analysis Program for Static and Dynamic Nonlinear Analysis of Framed Structures. Available at: <URL>
- Turan, A. I., Celik, A., Kumbasaroglu, A., & Yalciner, H. (2024). Assessment of reinforced concrete building damages following the Kahramanmaraş earthquakes in Malatya, Turkey (February 6, 2023). *Engineering Science and Technology, an International Journal*, 54, 101718. <https://doi.org/10.1016/j.jestch.2024.101718>
- TS 708, Turkish Standards Institute. (1973). TS 708-Steel for the reinforcement of concrete – reinforcing steel, Ankara.
- Vuran, E., Serhatoğlu, C., Timurağaoğlu, M. Ö., Smyrou, E., Bal, İ. E., & Livaoğlu, R. (2024). Damage observations of RC buildings from 2023 Kahramanmaraş earthquake sequence and discussion on the seismic code regulations. *Bulletin of Earthquake Engineering*, 23, 1153-1182. <https://doi.org/10.1007/s10518-023-01843-3>
- Wang, X., Feng, G., He, L., An, Q., Xiong, Z., Lu, H., Wang, W., Li, N., Zhao, Y., Wang, Y., & Wang, Y. (2023). Evaluating Urban Building Damage of 2023 Kahramanmaras, Turkey Earthquake Sequence Using SAR Change Detection. *Sensors*, 23(14), 6342. <https://doi.org/10.3390/s23146342>
- Zengin, B., & Aydin, F. (2023). The Effect of Material Quality on Buildings Moderately and Heavily Damaged by the Kahramanmaraş Earthquakes. *Applied Sciences*, 13(19) 10668. <https://doi.org/10.3390/app131910668>